Supporting Information

Interlaced Pd-Ag nanowires rich in grain boundary defects for boosting oxygen reduction electrocatalysis

Xiao-Jing Liu‡[a], Xing Yin‡[a], Yi-Dan Sun[a], Feng-Jiao Yu[a]*, Xiang-Wen Gao[b]*, Li-Jun Fu[a], Yu-Ping Wu[a] and Yu-Hui Chen[a]*

[a] *State Key Laboratory of Materials-oriented Chemical Engineering, School of Energy, Nanjing Tech University. Nanjing, Jiangsu, 211816, China*

[b] *Materials Science and Engineering Program and Department of Mechanical Engineering, The University of Texas at Austin, Austin 78712 TX, USA*

Methods

Chemical and Materials.

Palladium(II)-acetylacetonate [$Pd(acac)_2$] were received from sigma. $AgNO_3$, polyvinylpyrrolidone (PVP, MW 55,000), ethylene glycol, H_2SO_4, HNO_3, isopropanol, KOH were purchased from Shanghai Chemical Reagent Co. Ltd.

Materials Characterization.

Powder X-ray diffraction (XRD) was performed on a PANalytical Empyrean diffractometer with Cu K_α radiation. HRTEM images and selected area electron diffraction (SAED) patterns were obtained on a JEOL-2011 electron microscope operating at 200 kV equipped with an Oxford Link ISIS system for EDS. XPS was taken on Thermo ESCALAB 250XI with an X-ray source (Mg Kα $h\upsilon$ = 1253.6 eV).

Synthesis of Pd-Ag catalysts.

Pd_1Ag_1 nanowires were prepared via modified polyol process. In general, 30 mg of $Pd(acac)_2$, 17 mg of $AgNO_3$, 40 mg of polyvinylpyrrolidone (PVP, MW 55,000) were dissolved in 5 mL of ethylene glycol (EG). Under vigorous stirring, the mixture was heated to 80 ^oC until the solution was clear. The solution was further heated to 200 ^oC and refluxed for 2 h. The precipitate was centrifuged and washed with ethanol for several times.

Pd_4Ag_1 and Pd_1Ag_4 nanowires were synthesized via the same procedure above expect changing the mole ratio of Pd/Ag to 4/1 and 1/4 with the fixed total mole amount, respectively. Pd nanoparticle chains were obtained without the addition of $AgNO_3$ in the reaction.

Carbon nanotube (CNT) supported PdAg nanoparticles were prepared as below. CNTs were treated in acid to introduce more functional groups, which allows better and even growth of PdAg nanoparticles on the surface of carbon. Pristine CNTs were refluxed in the solution of concentrated H_2SO_4/ HNO_3/ H_2O (3/1/1 in volume) at 100 ^oC for 4 h, followed by washing with deionized water to neutrality. The functionalized CNTs were dispersed in EG under ultrasonication for 1 h. $Pd(acac)_2$, $AgNO_3$ and PVP were added into the CNT (1 mg/ mL) dispersion. The solution was refluxed at 200 ^oC for 2 h. The precipitate was centrifuged and washed with ethanol for several times.

Electrocatalytic measurements

PdAg catalysts were dispersed in 5 ml isopropanol aqueous (isopropanol/H_2O: 4:1) solution by ultrasonicating to form catalyst ink. For RDE, 10 µl of ink was dropped onto a polished glassy carbon (GC) electrode (5 mm diam.). The catalyst loading on glassy electrode was 25.5 µg cm^{-2}. 20 wt.% Pt/C catalyst (Johnson Matthey) with the same mass loading were tested for comparison.

Electrochemical studies were carried out on a potentiostat (CH instrument, Shanghai, China.) with a rotation control (Pine Ins.). A three-electrode cell was constructed with a GC working electrode (WE), a Hg/HgO reference electrode (RE) and a platinum foil counter electrode (CE). 0.1 M aqueous KOH solution was used as electrolyte and O_2 was bubbled at least for 30 minutes before measurements. Before measurement, all the catalysts were activated by cyclic voltammograms running CV scans from 0.05 to 1.20 V (*vs*. RHE) under N_2 flowing at a scan rate of 250 mV s^{-1} for 50 cycles. Linear sweep voltammetry measurement for ORR were performed in O_2 electrolyte with a scan rate of 10 mV s^{-1} (electrode rotating rate: 1600 rpm)

The long-term stability test was conducted in saturated 0.1 M KOH solution by cycling the potential from 0.6-1.0 V (*vs*. RHE) at 100 mVs^{-1} for 5000 cycles. The ORR polarization curves were then recorded after the potential cycling.

To evaluate the tolerance towards methanol, RDE electrodes with catalyst loading were held at 1600 rpm rotation in a 0.5 M methanol and 0.1 M KOH mixed solution, and the LSV were recorded at 10 mVs^{-1}.

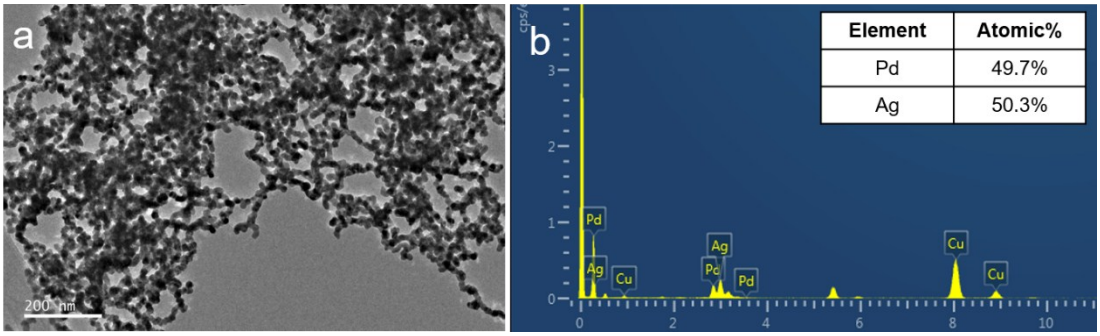

Fig. S1 (a) TEM image and (b) EDS result of the obtained Pt-Ag nanowires.

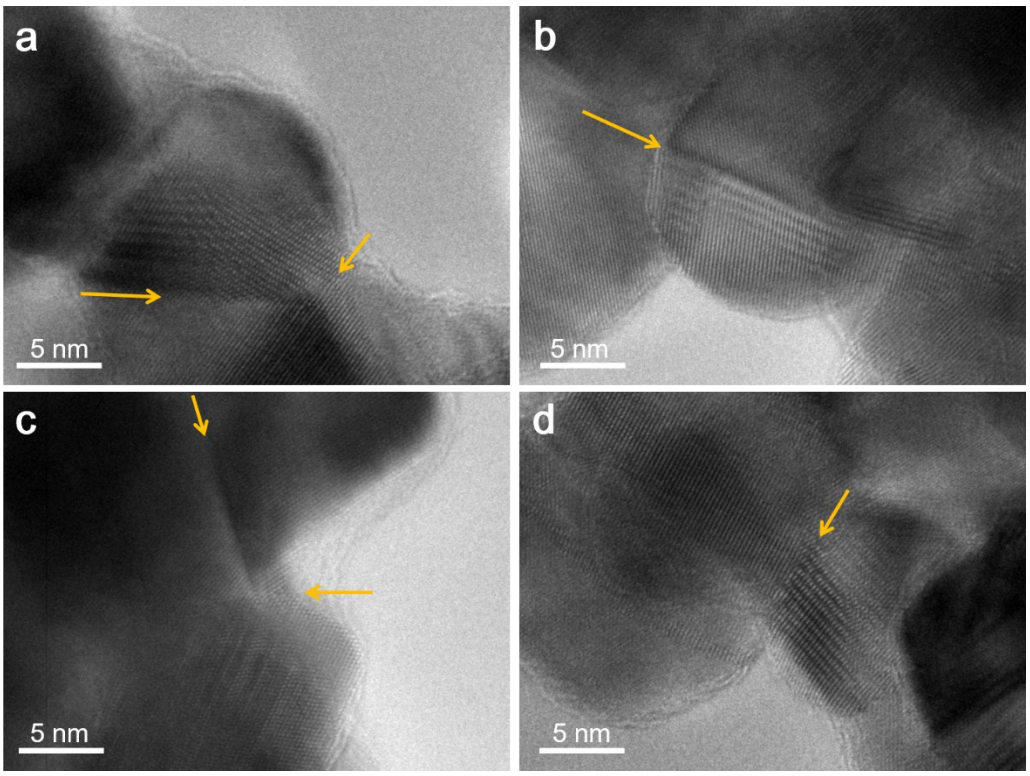

Fig. S2 (a-d) HRTEM images of Pd_1Ag_1 NWs.

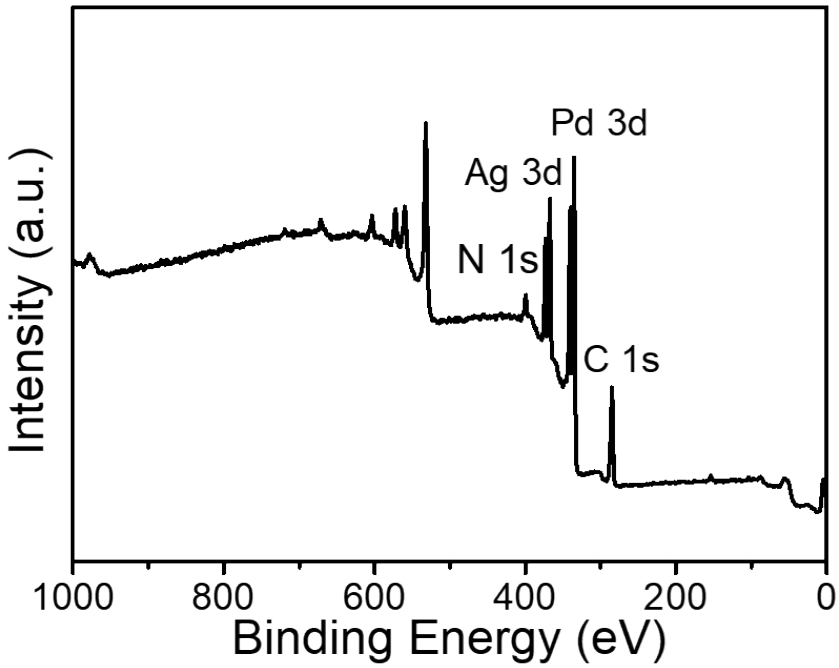

Fig. S3 XPS survey spectrum of Pd_1Ag_1 NWs.

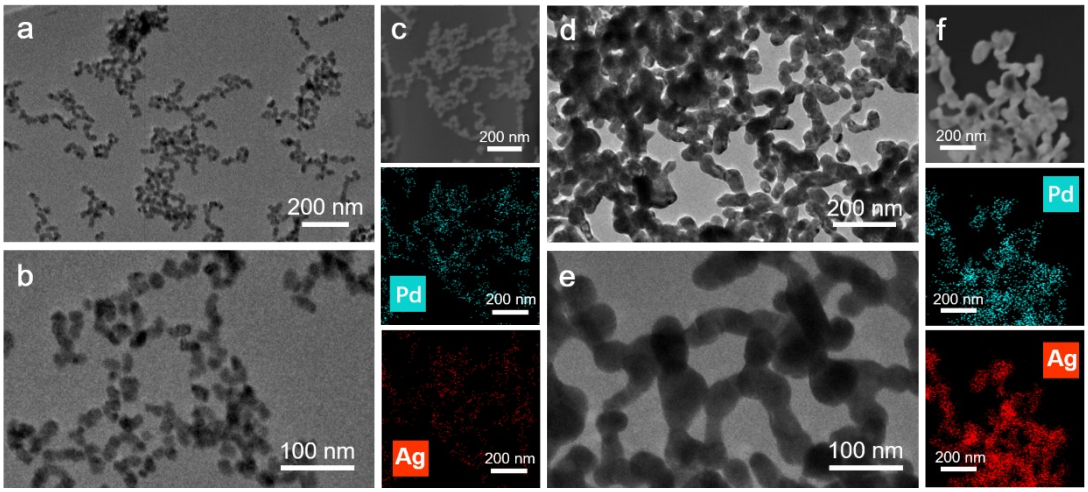

Fig. S4 (a, b) (d, e) TEM images of Pd_4Ag_1 and Pd_1Ag_4 NWs; (c, f) elemental mapping of Pd_4Ag_1 and Pd_1Ag_4 NWs, respectively.

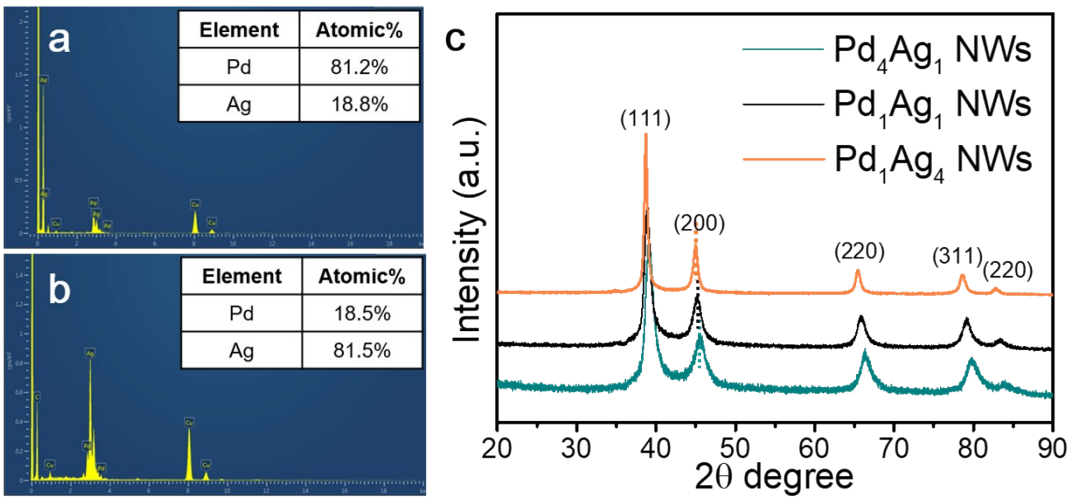

Fig. S5 (a-b) EDS and the corresponding element atomic ratio of Pd_4Ag_1 and Pd_1Ag_4 NWs. (C) XRD patterns of Pd_4Ag_1, Pd_1Ag_1 and Pd_1Ag_4 NWs.

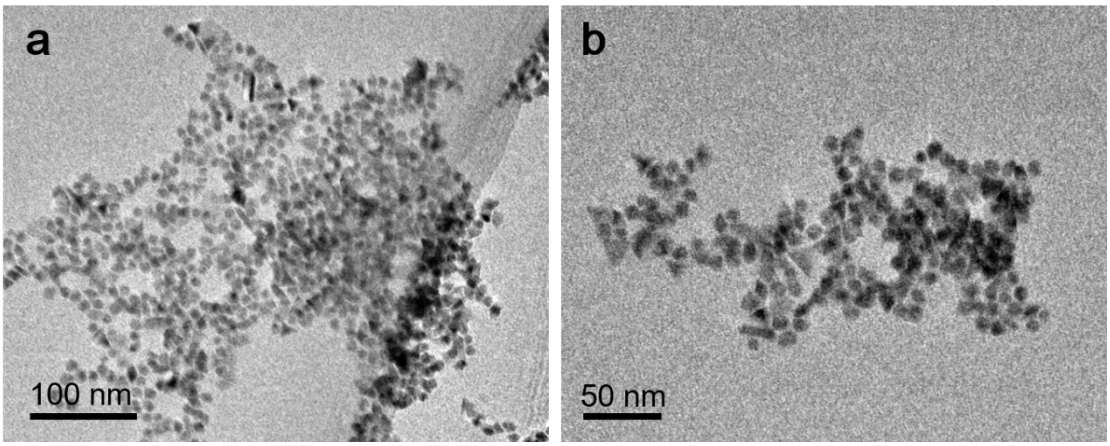

Fig. S6 TEM images of the product of without the addition of $AgNO_3$ in the reaction.

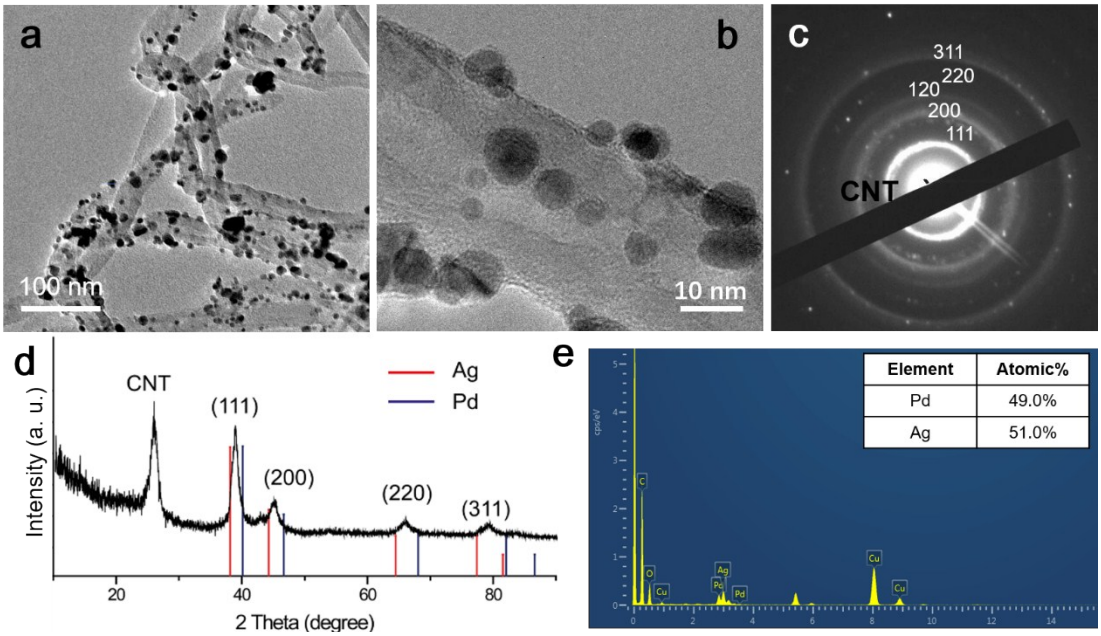

Fig. S7 (a-b) TEM image of carbon tubes supported PdAg nanoparticles; (c) the corresponding selected-area electron diffraction pattern; (d) XRD pattern; (e) EDS result.

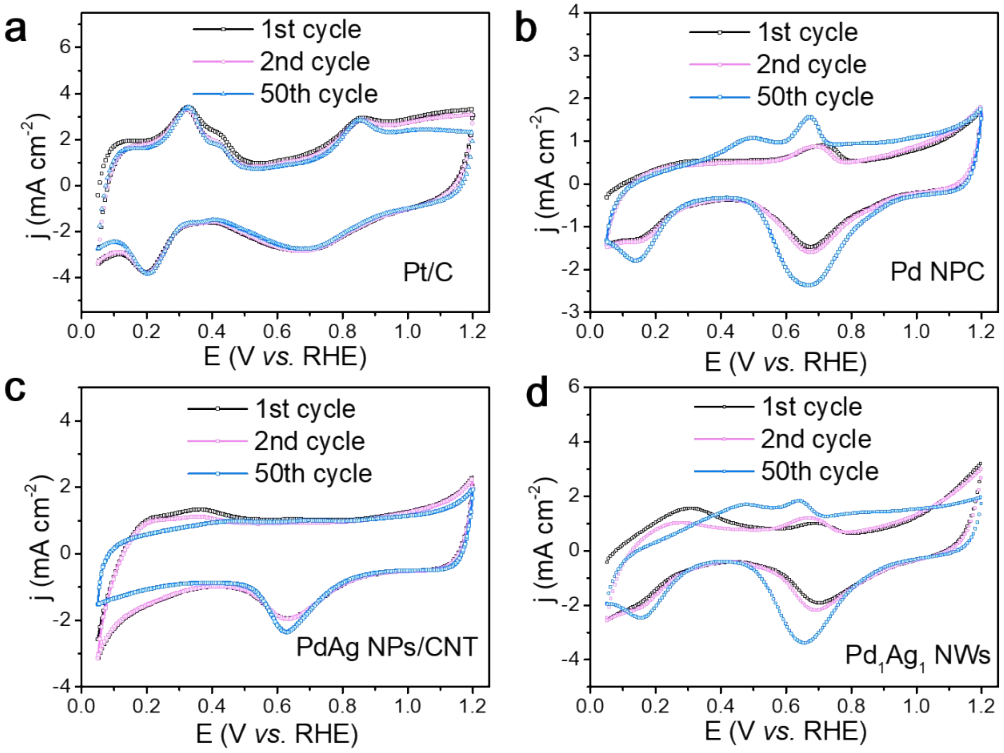

Fig. S8 (a-d) CV curves of the 1st, 2nd and 50th cycles of Pt/C, Pd NPC, PdAg NPs/CNT, and Pd_1Ag_1 NWs, respectively.

Catalysts	Electrolyte	Mass activity	Reference
AuPd NPs/RGOs	0.1 M KOH	0.015 A mg^{-1}_{Pd}	1
Ni@Pd3/C NPs	0.1 M KOH	0.038 A mg^{-1} (0.9V)	2
Pd nanocubes@Mo/C	0.1 M KOH	0.11A mg^{-1}_{Pd} (0.85V)	3
Pd-Ni/CNFO 1:2	0.1 M KOH	0.098 A mg^{-1} (0.85V)	4
PdNi Hollow Nanoparticles	0.1 M KOH	1.81×10^{-4} A mg^{-1}	5
Pd_6Sn_3Co intermetallic compounds	0.5M KOH	0.03 A mg^{-1} (0.9V)	6
CuPd/graphene	0.1 M KOH	0.045 A mg^{-1}_{Pd} (0.7V)	7
Pd-B/C	0.1 M KOH 0.1 M $HClO_4$	0.145 A mg^{-1}_{Pd} (0.9V) 0.055 A mg^{-1}_{Pd} (0.9V)	8
Ordered Pd_3Pb/C	0.1 M KOH	0.168 A mg^{-1}_{Pd}	9
$MnPd_3$/C	0.1 M KOH	0.051A mg^{-1} (0.75V)	10
CoAuPd-3 NCs	0.1 M KOH	0.082 A mg^{-1}_{Pd}	11
Pd_1Ag_1 NWs	0.1 M KOH	0.103 A mg^{-1}_{Pd} (0.9 V)	***This work***

Table S1 Comparison of the ORR performance of Pd_1Ag_1 NWs in alkaline medium with various Pd-based electrocatalysts previously reported.

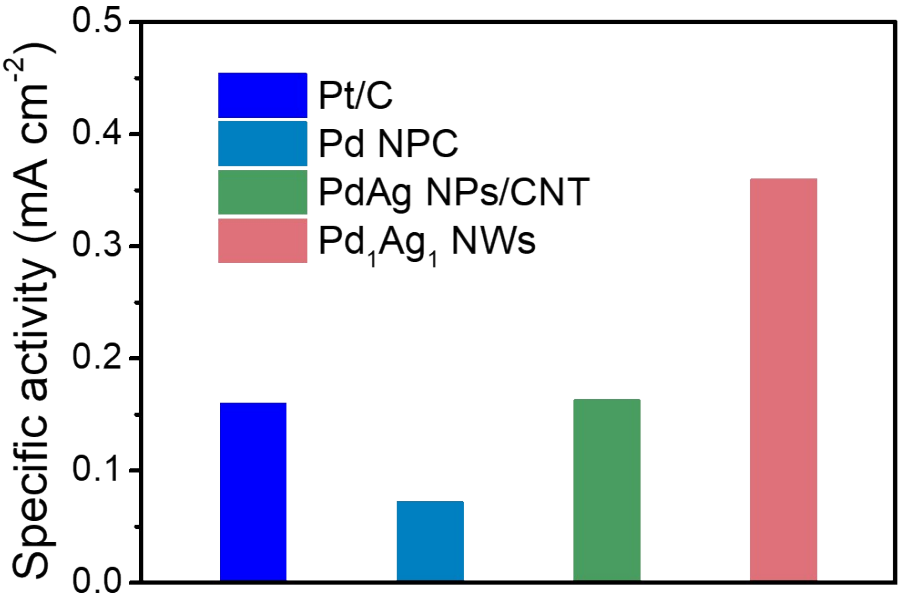

Fig. S9 Comparison of specific activities of Pd_1Ag_1 NWs, PdAg NPs/CNT, Pd NPC, and commercial Pt/C catalysts

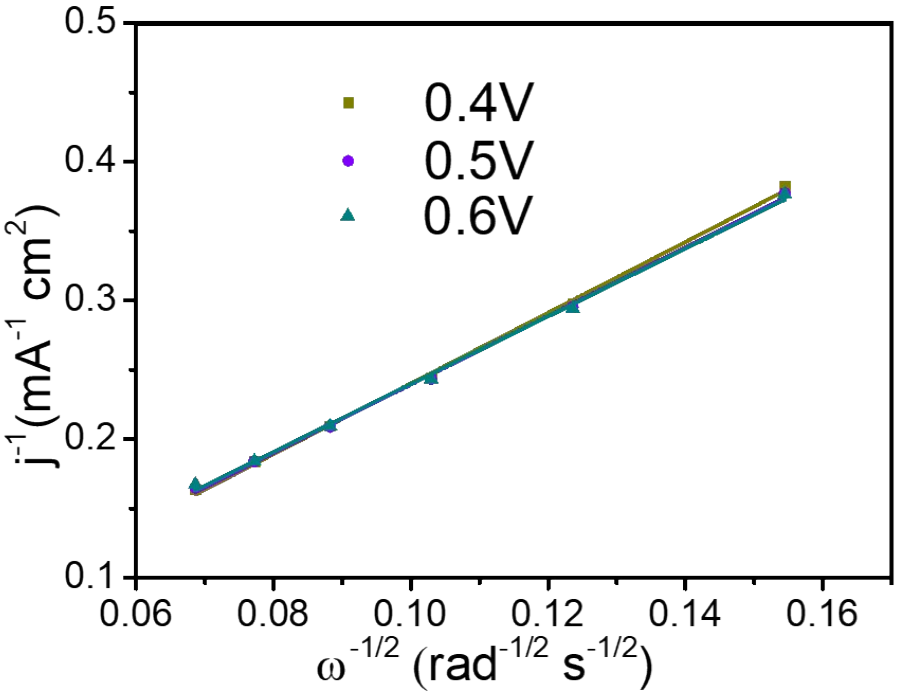

Fig. S10 Koutecky-Levich plots for the Pd_1Ag_1 NWs (j^{-1} vs. $\omega^{-1/2}$)

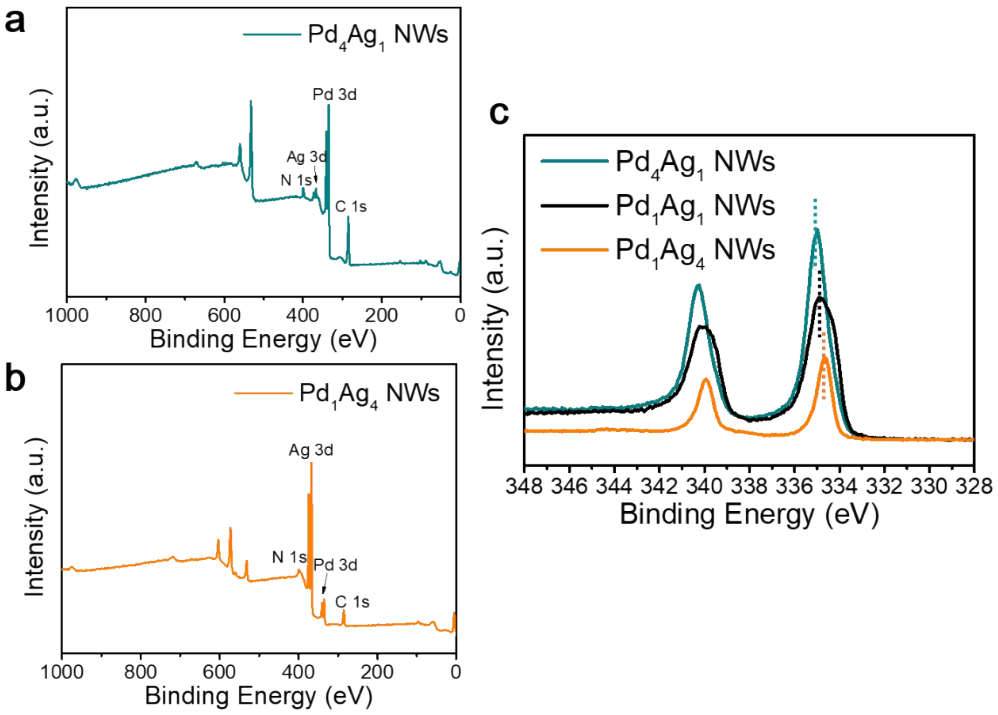

Fig. S11 (a, b) XPS survey spectrums of Pd_4Ag_1 and Pd_1Ag_4 NWs; (c) XPS spectra of Pd 3d region in Pd_xAg_y NWs with different Pd/Ag ratio (Pd_4Ag_1, Pd_1Ag_1, Pd_1Ag_4).

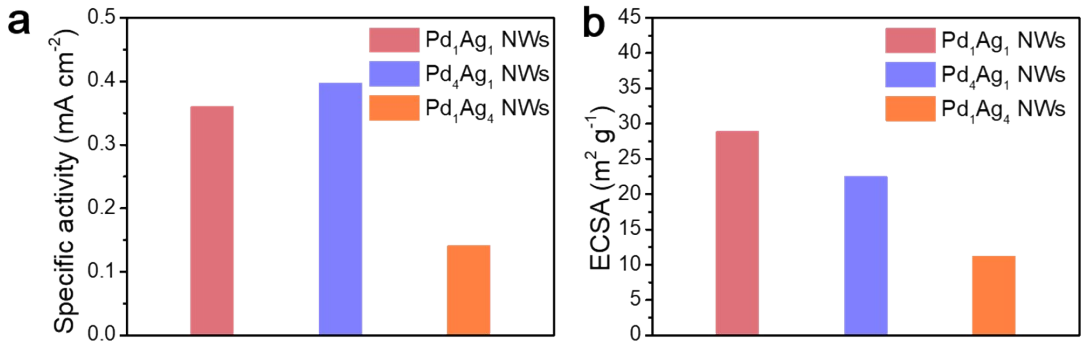

Fig. S12 Comparison of specific activities and ECSAs of Pd_1Ag_1, Pd_4Ag_1, and Pd_1Ag_4 NWs.

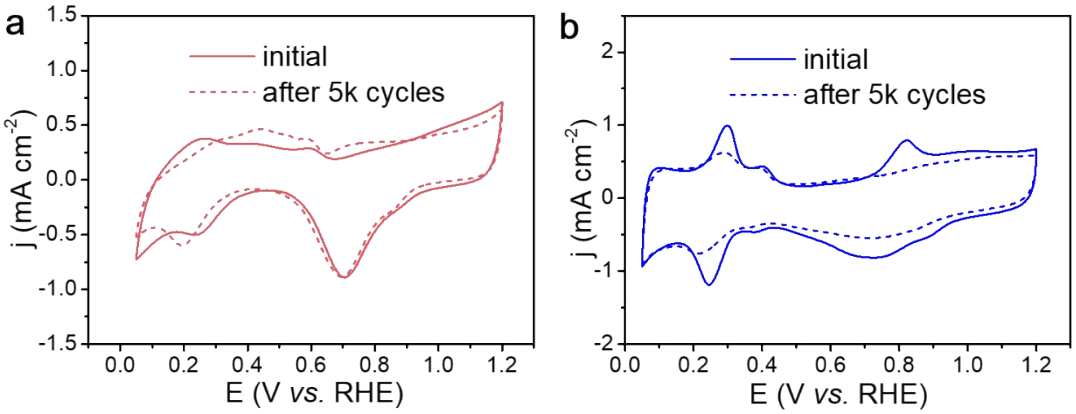

Fig. S13 (a, b) CV of Pd_1Ag_1 NWs and commercial Pt/C catalyst recorded in N_2-saturated 0.1 KOH solution at 50 mVs^{-1} before (the solid curve) and after (the dashed curve) stability test.

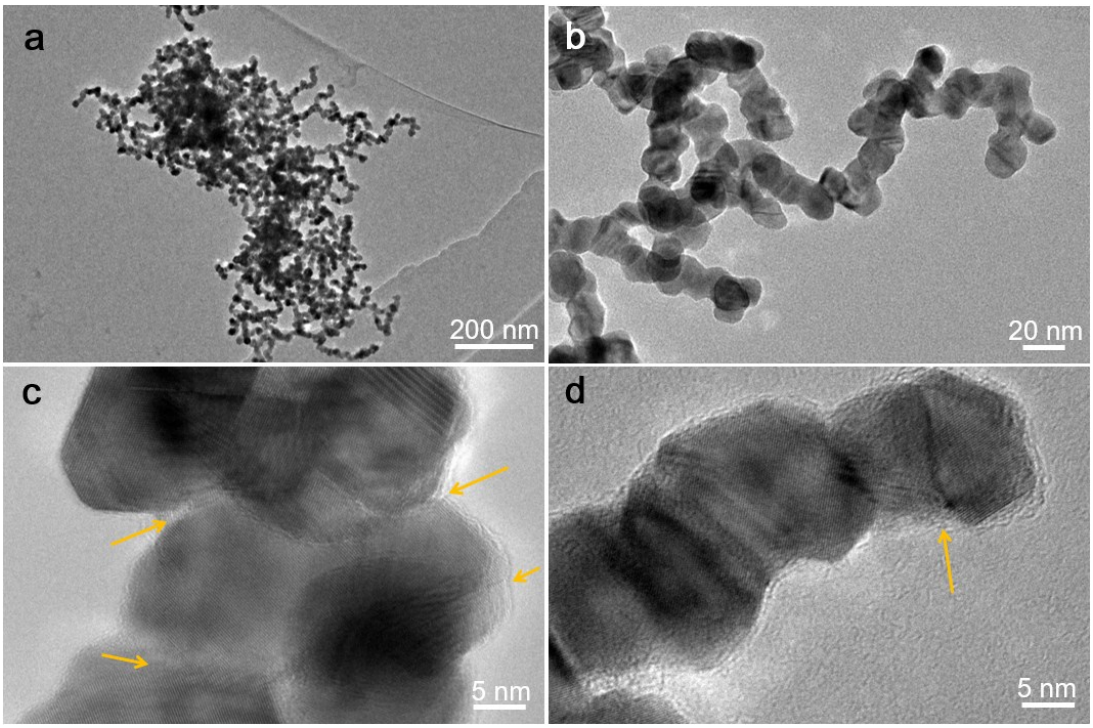

Fig. S14 TEM (a, b) and HRTEM images (c, d) of Pd_1Ag_1 NWs after stability test.

Reference

1. J. J. Lv, S. S. Li, A. J. Wang, L. P. Mei, J. R. Chen and J. J. Feng, *Electrochim. Acta* 2014, **136**, 521-528.
2. J. Jiang, H. Gao, S. Lu, X. Zhang, C. Y. Wang, W. K. Wang and H. Q. Yu, *J. Mater. Chem. A*, 2017, **5**, 9233-9240.
3. W. Yan, W. Wu, K. Wang, Z. H. Tang and S. W. Chen, *Int. J. Hydrogen Energy* 2018, **43**, 17132-17141.
4. J. C. Calderon, V. Celorrio, M. J. Nieto-Monge, D. J. Fermin, J. I. Pardo, R. Moliner and M. J. Lazaro, *Int. J. Hydrogen Energy* 2016, **41**, 22538-22546.
5. M. Wang, W. Zhang, J. Wang, D. Wexler, S. D. Poynton, R. C. T. Slade, H. Liu, B. Winther-Jensen, R. Kerr, D. Shi and J. Chen, *ACS Appl. Mater. Interfaces* 2013, **5**, 12708-12715.
6. Y. Wu, C. Wang, L. Zou, Q. Huang and H. Yang, *J. Electroanal. Chem.* , 2017, **789**, 167-173.
7. Y. Zheng, S. Zhao, S. Liu, H. Yin, Y.-Y. Chen, J. Bao, M. Han and Z. Dai, *ACS Appl. Mater. Interfaces* 2015, **7**, 5347-5357.
8. M. Wang, X. Qin, K. Jiang, Y. Dong, M. Shao and W.-B. Cai, *J. Phys. Chem. C*, 2017, **121**, 3416-3423.
9. Z. Cui, H. Chen, M. Zhao and F. J. DiSalvo, *Nano Lett.* , 2016, **16**, 2560-2566.
10. Y. Lu, S. Zhao, R. Yang, D. Xu, J. Yang, Y. Lin, N.-E. Shi, Z. Dai, J. Bao and M. Han, *ACS Appl. Mater. Interfaces* 2018, **10**, 8155-8164.
11. L.-M. Luo, W. Zhan, R.-H. Zhang, D. Chen, Q.-Y. Hu, Y.-F. Guo and X.-W. Zhou, *J. Power Sources* 2019, **412**, 142-152.